Ultrasound-responsive matters for biomedical applications
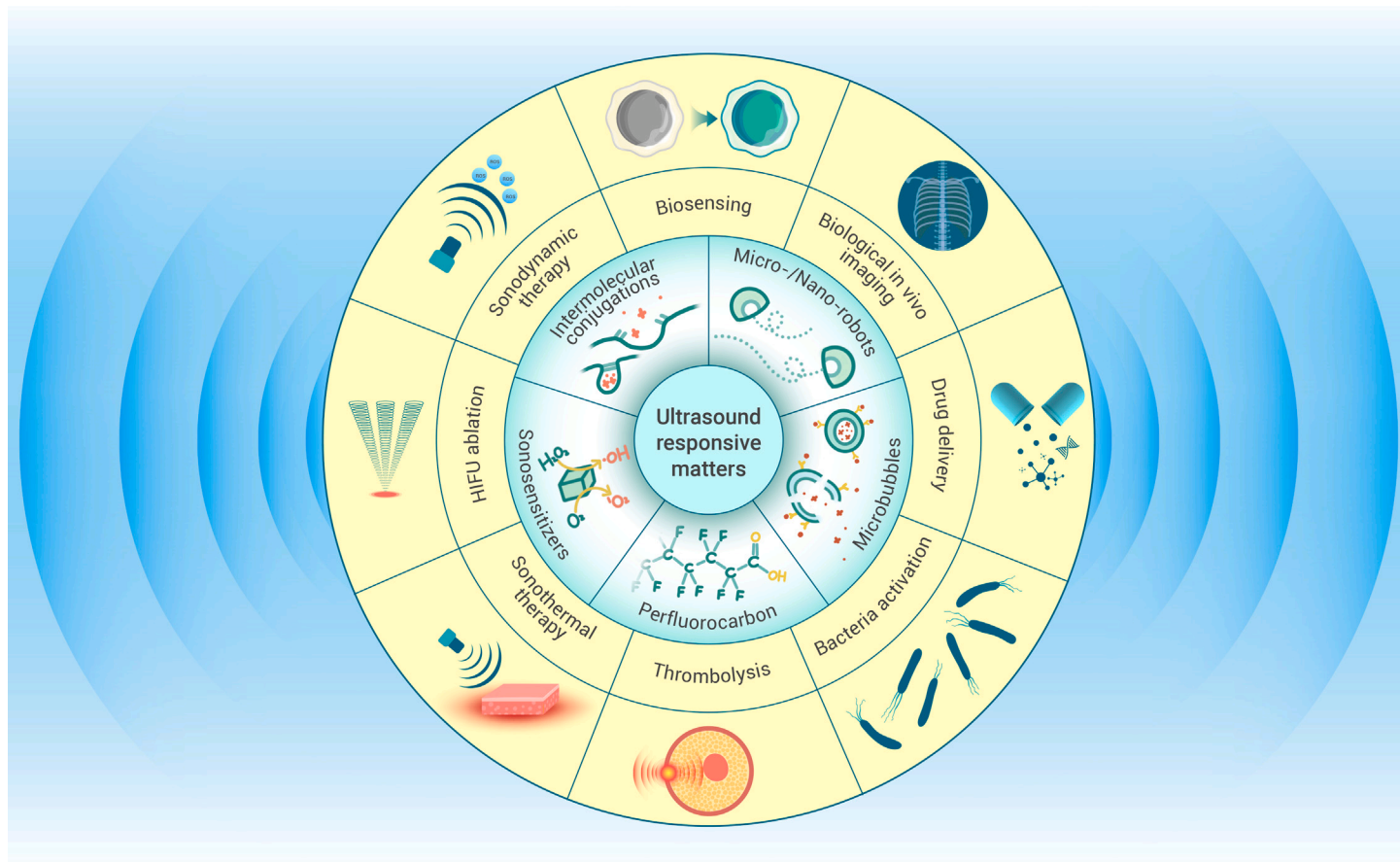
Danqing Huang,[1] Jinglin Wang,[1] Chuanhui Song,[1] and Yuanjin Zhao[1,2,3,*]

*Correspondence: yjzhao@seu.edu.cn

GRAPHICAL ABSTRACT

PUBLIC SUMMARY

- Ultrasound is a biofavorable mechanical wave with broad application potentials.

- Various ultrasound-responsive matters have been explored.

- These advanced matters have bight future in multidisciplinary fields.

Ultrasound-responsive matters for biomedical applications

Danqing Huang,[1] Jinglin Wang,[1] Chuanhui Song,[1] and Yuanjin Zhao[1,2,3,*]

[1]Department of Rheumatology and Immunology, Institute of Translational Medicine, The Affiliated Drum Tower Hospital of Nanjing University Medical School, Nanjing 210002, China
[2]State Key Laboratory of Bioelectronics, School of Biological Science and Medical Engineering, Southeast University, Nanjing 210096, China
[3]Chemistry and Biomedicine Innovation Center, Nanjing University, Nanjing 210023, China
*Correspondence: yjzhao@seu.edu.cn

Ultrasound (US) is a biofavorable mechanical wave that has shown practical significance in biomedical fields. Due to the cavitation effect, sonoluminescence, sonoporation, pyrolysis, and other biophysical and chemical effects, a wide range of matters have been elucidated to be responsive to the stimulus of US. This review addresses and discusses current developments in US-responsive matters, including US-breakable intermolecular conjugations, US-catalytic sonosensitizers, fluorocarbon compounds, microbubbles, and US-propelled micro- and nanorobots. Meanwhile, the interactions between US and advanced matters create various biochemical products and enhanced mechanical effects, leading to the exploration of potential biomedical applications, from US-facilitated biosensing and diagnostic imaging to US-induced therapeutic applications and clinical translations. Finally, the current challenges are summarized and future perspectives on US-responsive matters in biomedical applications and clinical translations are proposed.

INTRODUCTION

Acoustic waves are a form of mechanical vibration that propagates through a medium via the mechanical compression and rarefaction of matter. The frequencies of acoustic waves are broad, spanning from less than 1 Hz to over 100 GHz.[1] Among these, ultrasound (US) refers to acoustic waves with frequencies that exceed the upper limit of human hearing (20 kHz). Due to its ability to propagate through various materials with low losses and short time scales, US has attracted multidisciplinary research interests. In particular, the exploration of US-responsive matters has enhanced US's potential in practical applications, including effective energy transfer and the sensitive interaction with microscale systems. Generally, human tissue is a kind of US-responsive matter, as clinicians have discovered that periodic US pulses can cause corresponding vibrations of biological tissues. The reflection of these vibrations can be detected through piezoelectric elements, paving the way for the establishment of ultrasonography. With significant advancements in US transducers, different US frequencies and excitation pressures can now be generated through the conversion from electrical energy to mechanical vibrations. As a result, various ultrasonography modes have been developed and employed for biological imaging.

Clinically, US has been a well-established diagnostic modality in medical imaging due to its real-time property, high permeability, and lack of radiation.[2–7] Its advanced development has contributed significantly to clinical applications for the imaging of more biophysical information. One example is color Doppler flow imaging (CDFI), which utilizes the Doppler effect between red blood cells and US to show the blood flow of the human body. Two-dimensional ultrasonography provides the anatomical structure of the human body, and the combination of both techniques provides complete anatomical information, contributing to the clinical evaluation of blood distribution, flow direction, and velocity.[8,9] In contrast, share-wave elastography is another emerging US imaging technique that manipulates the acoustic radiation force produced by an ultrasonic beam to perturb the tissue.[10] Elastic media such as human tissue respond to this push because of its own restorative force, thus causing mechanical waves that can be used to quantitatively display the hardness of human soft tissue.[9] Share-wave technology has been applied in medical imaging by medical engineers in recent years, offering a promising tool for tissue characterization. Typically, liquid containing bubbles has the characteristic of strong scattering properties of US, leading to the development of contrast-enhanced US (CEUS). Through the injection of microbubbles into human blood vessels, the US Doppler signal of blood flow can be significantly enhanced, contributing to the improvement of the clarity and resolution of ultrasonographies.[11–14]

Among the many diagnostic techniques available, US has gained significant attention due to its mechanical waves with potential for therapeutic applications. In addition to its diagnostic value, the US-induced cavitation effects of contrast-enhancing agents, such as microbubbles, have been extensively studied for their ability to enhance endovascular contrast-enhanced imaging, navigate drug delivery, and trigger drug release. Furthermore, US-induced cavitation combined with mechanical energy conversion has led to the discovery of high-intensity focused US (HIFU) ablation, a noninvasive and nonradiative ablation therapy with promising applications in treating Alzheimer's disease and tumors. In contrast, sonodynamic therapy (SDT), based on the combination of low-intensity US and sonosensitizer hematoporphyrin, has shown tremendous potential in managing diseases.[15] The use of US-sensitive agents, including organic and inorganic sonosensitizers, has further facilitated SDT. Nowadays, various clinical trials for US-based disease management are currently underway.[16,17]

This review aims to provide a comprehensive overview of the mechanisms underlying the interactions between US and various matters and to highlight the practical significance of US-responsive substances in biomedical applications. This review first discusses the established mechanisms of US-matter interactions, including the cavitation effect, sonoluminescence, sonoporation, and thermal effects. Then, various US-responsive matters with promising practical significance are introduced, such as intermolecular conjugations that can be broken by US, sonosensitizers that generate free radicals upon US excitation, fluorocarbon compounds that can undergo liquid-to-gas phase transition under US excitation, microbubbles that expand and explode through US irradiation, and micro- and nanorobots that can be propelled and navigated by US. Meanwhile, we cast light on the potential biomedical applications of the US-responsive substances in both diagnostic and therapeutic settings. Finally, the challenges being faced are summarized to make a forecast for the future biotechnological applications and clinical translations of US-responsive matters.

US-INDUCED MECHANISMS

Currently, US with a frequency between 1 and 20 MHz is widely applied in real-time imaging, and US with a frequency between 0.7 and 3.3 MHz has shown practical significance in rehabilitation medicine. With the assistance of a transducer that can transmit US of specific frequency and power, US can penetrate the skin of patients, targeting deep seated tissue with low attenuation to realize the desired efficacy, such as assessing tissue condition, relaxing connective tissues, etc. In recent decades, US has also been discovered to have therapeutic effects in anticancer treatments, and various US-matter interaction mechanisms have been explored. Cavitation effects are the most representative and plausible mechanisms, including stable and inertial cavitation. Cavitation refers to the nucleation of gas bubbles when the US interacts with liquid and plays a nonnegligible role in US-based treatments.

According to the different frequencies and powers of the US pulses, cavitation includes stable cavitation and inertial cavitation. Generally, stable cavitation, also known as the noninertial cavitation, refers to the oscillation of bubbles. Therefore, stable cavitation usually leads to the microstreaming of the surrounding aqueous environment. When stable cavitation occurs in tissue, the microstreaming caused by the stable cavitated bubbles further leads to friction between the gas bubbles and the tissue, along with the oscillation of the tissues. Thus, the acoustic energy is converted to heat energy, increasing the temperature of tissues, which is known as the thermal effect of US. In contrast, inertial cavitation refers to the rapid expansion of bubbles, which continue to expand until they reach resonance size, and the subsequent impulsive collapse. During the savage burst of these cavitation bubbles, a great deal of heat and pressure energy is generated due to the conversion of mechanical energy.[18]

A

Inactive

Active

B

Drug deactivation

Inactive

Active

C

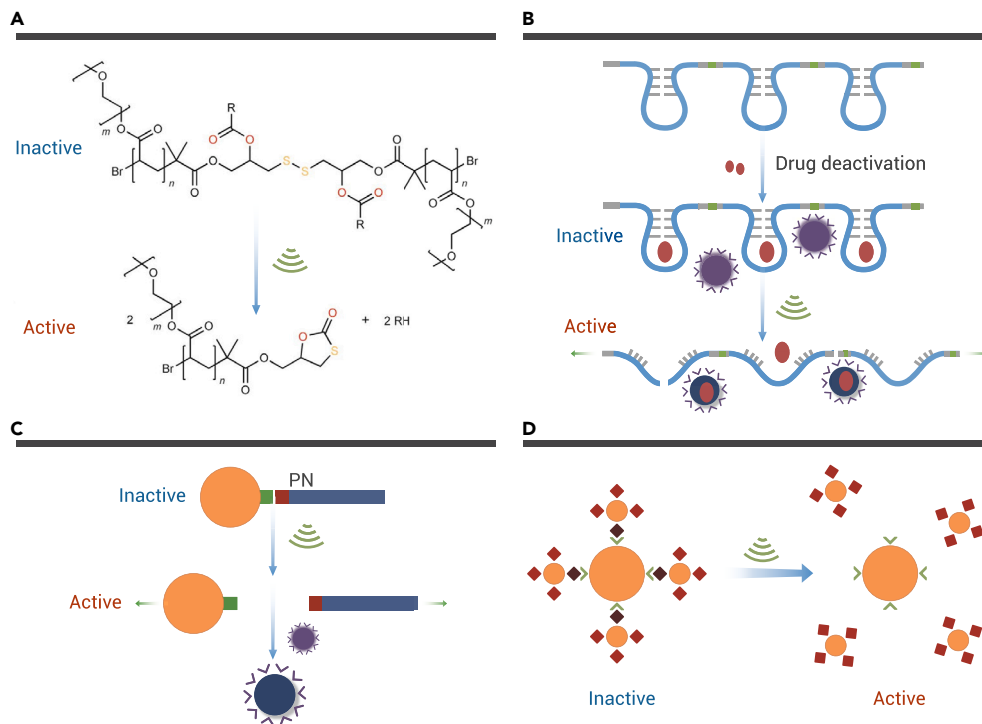
Inactive

PN

Active

D

Inactive

Active

Figure 1. The US-mediated mechanoresponsive prodrug systems (A) Schematic illustration of the molecular structure before and after US activation. (B) Schematic illustration of the US-mediated release of RNA polyaptamer-encased neomycin B. (C) Schematic diagram of US-activated Au-DADA + $P_{van}s$. (D) Schematic diagram of nanoparticle-nanoparticle assemblies.[31] Copyright 2021, Springer Nature.

when it is required to send microbubbles into a narrower tumor interstitial space without destroying their stability, US-induced phase-change substances are being explored. According to the thermal effect caused by US, thermosensitive and thermoresponsive materials are applied to fabricate US-responsive intelligent drug carriers. In recent decades, to enhance the therapeutic efficacy of SDT and HIFU ablation, great efforts have been focused on the discovery and synthesis of smart agents that can increase ROS production and hyperthermia.[23–30] Therefore, diverse US-responsive matters, including US-breakable intermolecular conjugations, ROS-producing materials, fluorocarbon compounds with phase-transiting properties, lipid or hydrogel microbubbles, and micro- and nanorobots, along with their potential practical applications, will be addressed here through typical examples.

Based on the extreme heat caused by inertial cavitation, some other effects, such as sonoluminescence and pyrolysis, occur. Sonoluminescence refers to the generation of light during the US-mediated cavitation effect. Umemura and co-workers described an emission of light with a peak of approximately 450 nm from the interaction between US and saline solutions.[19] The light activated by US can trigger the production of reactive oxygen species (ROS) in the presence of sonosensitizers, most of which originate from photosensitizers. The mechanism of US-excited light generation has not been documented exactly; numerous hypotheses have been proposed, including bremsstrahlung, recombination radiation, blackbody, and so on. Pyrolysis involves the generation of ROS when the sonosensitizers get broken up under inertial cavitation-caused extreme heat. The generated ROS can lead to cancer cell apoptosis through lipid peroxidation and other biological effects.[20] Meanwhile, according to the pressure derived from the violent collapse of cavitated bubbles, which reaches 81 MPa,[20] reversible micropores appear on the cell membranes, the process of which is referred to as the sonoporation effect. The sonoporation effect of US benefits the inflow of extracellular drugs, thus enhancing the drug uptake efficiency of targeted cells, minimizing the drug residue in normal tissues, and increasing the therapeutic effect.[21,22]

To summarize, US is a mechanical wave with low attenuation and high spatial accuracy in human tissue. As the most important and commonly accepted mechanism of US-based treatments, cavitation effect refers to the generation and oscillation of cavitated gas bubbles. The resultant high temperature and pressure caused by the violent collapse of cavitated gas bubbles would subsequently trigger more effects, such as thermal effect, sonoluminescence effect, pyrolysis, and sonoporation effect. Although the exact mechanism requires more investigations, the therapeutic efficacy of US-based treatments is well established.

US-RESPONSIVE MATTERS AND POTENTIAL APPLICATIONS

The mechanical and biophysical effects of US waves make them potential candidates for therapeutic applications. For example, in tumor tissues exposed to US, cavitation bubbles can be produced in the liquid of the tumor tissues. As the bubbles expand and burst, the tumor tissues would be affected by the resultant microjet from inertial cavitation and other attendant effects. Despite the destructive effects that cause tumor cell damage, the limited amount of the cavitation bubbles produced by simple US wave severely hampers the antitumor efficacy. Thus, to enlarge the practical and therapeutic effects of US waves, US-responsive matters play an indispensable role. To ease the cavitation effect, artificial microbubbles are introduced into the human body. Moreover,

Intermolecular conjugations

By regulating the frequency and intensity of US waves, US can easily penetrate tissue and accurately target deep positions due to their temporal and spatial resolution. According to the specific mechanochemistry properties of some polymers, they can be transformed on the molecular level under US irradiation, such as the scissoring of intermolecular covalent and noncovalent bonds. The mechanical force of US exerts considerable effects on selectively targeting functional molecular motifs to trigger drug release. One area of research worth mentioning is reported by Huo's group, who explored three novel US-responsive prodrug systems that consisted of macromolecules or nanoassemblies.[31] The first prodrug platform was a polymer featuring a disulfide center (Figure 1A). By the covalent attachment of camptothecin (CPT) to the disulfide-centered polymer through a connection between carbonate at the β site of CPT and the disulfide moiety of the polymer, the CPT exhibited inactivity before US irradiation. Researchers elucidated that, after 4 h of US irradiation (frequency of 20 kHz), the CPT could be extruded from the carbonate linker of the anchored polymer. In vitro studies based on HeLa cells showed that the cell viability would decrease with the increase in US irradiation, illustrating the US-mediated bond scission of macromolecules and US-induced activation of drugs. The second prodrug system presented by Huo et al. used antibiotics bound to RNA polyaptamers, which were obtained from the transcription of a template containing the R23 RNA aptamer (Figure 1B).[31] The RNA polyaptamers showed a strong connection with antibiotics such as neomycin B and paromomycin. As introduced by the researchers, US could destroy the hydrogen bonds, electrostatic interactions, or other noncovalent and covalent interactions and bring about the collapse of the RNA backbone, thus activating the antibiotics. In agar plates culturing *Staphylococcus aureus*, it was demonstrated that the RNA polyaptamer-bound antibiotics had no antibacterial effect before US treatment. Notably, neomycin B carried by RNA polyaptamers exhibited a significant bacteria killing property only after US irradiation.

As reported by Huo et al., the third US-mediated mechanoresponsive prodrug regime was nanoparticle assemblies (Figure 1C).[31] These assemblies were based on a supramolecular motif, which was between the antibiotic vancomycin and a Cys-Lys-Lys(Ac)-d-Ala-d-Ala (DADA) sequence. Furthermore, the above-mentioned supramolecular motif can be used to either incorporate polymer chains with gold nanoparticles or connect multiple gold nanoparticles. By decorating gold nanoparticles with DADA (Au-DADA), the Au-DADA can be further
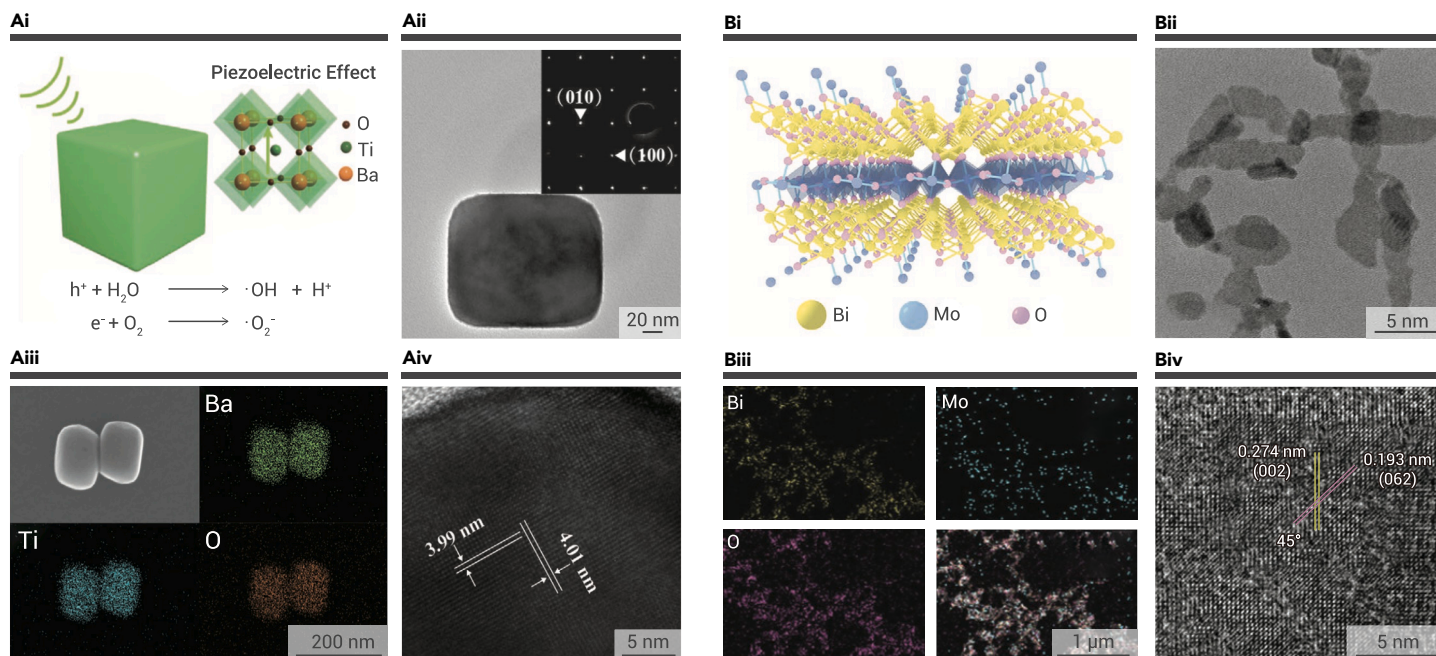
Figure 2. Inorganic sonosensitizers (A) The sonodynamic piezoelectricity of T-BTO. (i) Schematic illustration of the piezoelectric mechanism for the T-BTO-based ROS generation. (ii–iv) Transmission electron microscopy (TEM) (ii), scanning electron microscopy (SEM) and corresponding elemental mapping (iii), and high-resolution TEM (HRTEM) (iv) images of T-BTO.[46] Copyright 2020, WILEY-VCH. (B) The sonodynamic piezoelectricity of BMO. (i) Schematic illustration of the 2D structure of BMO. (ii–iv) TEM (ii), EDS elemental mapping (iii), and HRTEM (iv) images of BMO.[47] Copyright 2021, Wiley-VCH.

decorated with polymer-terminated vancomycin (Au-DADA + P_{van}), thus establishing a nanoparticle assembly. Notably, researchers further fabricated nanoparticle-nanoparticle assemblies by incorporating vancomycin-decorated gold nanoparticles with smaller size (d = 8 nm) and DADA-decorated gold nanoparticles with larger size (d = 55 nm) (Figure 1D). *In vitro* experiments illustrated that both nanoparticle assemblies had excellent antibacterial effects on *S. aureus* only under the irradiation of US, indicating the feasibility and efficiency of the mechanochemical activation of US. Another study introducing US-mediated intermolecular conjugation destruction was reported by Sun and co-workers, who conjugated the sonosensitizer meso-tetra(4-carboxyphenyl) porphine (T790) to functional nanocomposites. The conjugation can be broken under US irradiation, contributing to the stability of T790 and the maintenance of nanocomposites' functions.[32] This way of mechanochemically activating drugs is of great novelty and significance, paving the way for the exploration of the new field referred to as "sonopharmacology."

Sonosensitizers

SDT has shown certain advantages in anticancer treatment, which is mainly based on the resultant ROS produced from the interaction between low-intensity US (LIUS) and sonosensitizers.[26,33] Initially, SDT developed from photodynamic therapy (PDT), which applied light with particular wavelength to excite photosensitizers to produce ROS. In addition, most of the sonosensitizers applied nowadays are derived from photosensitizers.[34] However, compared with PDT, SDT showed significant advantages in penetration depth and biosafety. Since numerous sonosensitizers were derived from photosensitizers, the inevitable phototoxicity caused by light exposure severely hampered their practical applications.[20,26,35] Thus, more and more sonosensitizers with enhanced biocompatibility and ROS productivity have been explored and synthesized, including organic, inorganic, and composite sonosensitizers. The exact mechanisms of the ROS production remain unclear, while various hypotheses suggest that it may be related to the cavitation effect.[36,37] When the US-induced cavitation effect occurs, a sonoluminescence effect, which refers to the generation of light from the interaction between US and fluid, subsequently happens. Umemura et al. discovered that the resultant light caused by the sonoluminescence effect could be absorbed by hematoporphyrin, which is a kind of photosensitizer.[19] After absorbing energy, the sonosensitizer was excited to a higher energy state, and when the US irradiation stopped, the high-energy-level sonosensitizer released the energy and recovered to ground state. The converted acoustic energy was subsequently transferred to the surrounding oxygen and brought about the gen-

eration of ROS, which can bring damage to tumor cells and bacteria through oxidative reactions. In the following sections, we present the organic, inorganic, and composite sonosensitizers, from those derived from photosensitizers to those synthesized and discovered recently.

Organic sonosensitizers. Most of the organic sonosensitizers originated from photosensitizers, such as porphyrins, xanthenes, and other organic molecules. Generally, porphyrins include hematoporphyrin, protoporphyrin IX (PpIX), sinoporphyrin sodium (DVDMS), chlorin e6 (Ce6), etc.; xanthenes include rose bengal (RB), erythrosine B, RB derivatives, etc. Phenothiazine compounds include promethazine hydrochloride, dioxopromethazine hydrochloride, methylene blue, etc.; fluoroquinolone antibiotics include levofloxacin, sparfloxacin, gatifloxacin, etc.; natural sonosensitizers include curcumin, hypericin, artesunate, etc.; and other organic small molecules include δ-aminolevulinic acid (ALA), indocyanine green (ICG), etc.[34] These organic sonosensitizers feature desired properties for SDT application. For example, the definite molecular structures of the organic sonosensitizers enable feasible reproducibility and large-scale production, and their sensitivity to low-intensity and low-frequency US avoids the hyperthermal and mechanical adverse effects caused by high-intensity or high-frequency US. Meanwhile, the organic sonosensitizers show excellent biocompatibility and biodegradability; combined with the biosafety and penetrability of US, organic sonosensitizers have shown promising potential in treating deep-located lesions. For example, ICG, which is a Food and Drug Administration-approved fluorescence indicator, exhibits excellent US sensitivity and has been described as having therapeutic effects against rheumatoid arthritis (RA).[38,39] Curcumin, a kind of natural sonosensitizer, has been described as having special sonodynamic therapeutic effects in inducing macrophage apoptosis and treating atherosclerosis when applied as a hydroxyl-conjugated form.[40,41] However, since the photosensitizers are sensitive to light, most of the organic sonosensitizers feature phototoxicity, which might cause excessive production of ROS, resulting in unavoidable oxidative damage. Moreover, most of the organic sonosensitizers feature poor water solubility, leading to aggregation in the blood circulation and low tumor targeting properties, thus limiting the antitumor efficacy.

Inorganic sonosensitizers. In addition to the traditional organic sonosensitizers, inorganic sonosensitizers, including titanium dioxide (TiO_2) nanoparticles, silicon nanoparticles, and gold (Au) nanoparticles, have also been explored for SDT.[42–45] Compared with organic sonosensitizers, inorganic sonosensitizers produce relatively less ROS under US excitation, while they feature more maneuverable structures and enhanced chemical stability. Recently, the piezoelectric nanomaterials have been described as ideal sonosensitizers. Take the
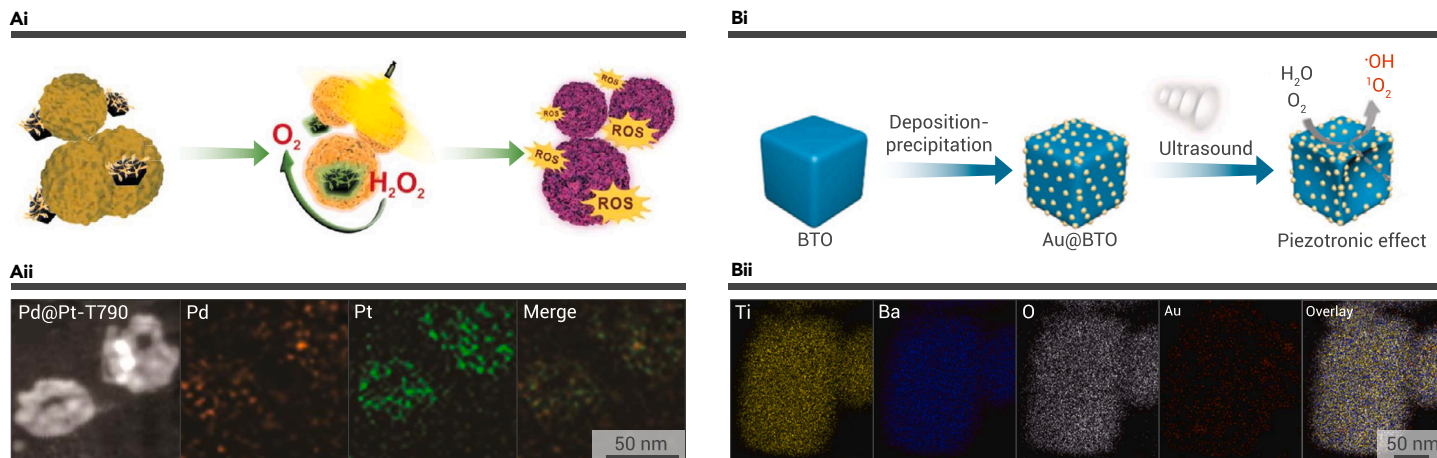
Figure 3. The US-responsive nanocomposites (A) Pd@Pt-T790 nanocomposites. (i) Schematic illustration of the US-activated oxygen and ROS generation of Pd@Pt-T790. (ii) SEM and X-ray spectroscopy mapping images of Pd@Pt-T790.[32] Copyright 2020, American Chemical Society. (B) The piezoelectric nanocomposite Au@BTO. (i) Scheme of the fabrication process and ROS-generating mechanism of Au@BTO. (ii) The elemental mapping of Au@BTO.[54] Copyright 2021, Elsevier.

noncentrosymmetric tetragonal barium titanate (T-BTO), for instance; it features near-cubic morphology and interplanar spacing, referring to the (100) and (001) planes (Figure 2A).[46] The periodic vibration of US pulses (1.0 MHz, 1.0 W cm^{-2}, 50%) can cause the excitation of the pressure-induced polarization of T-BTO, bringing about the establishment of a strong built-in electric field. The electric field subsequently leads to the separation of electrons and holes, which then attach to the opposite surface of T-BTO, and the piezocatalytic reaction occurs, leading to the generation of ROS. Bismuth molybdate (Bi_2MoO_6S, BMO) nanoribbon is another excellent piezoelectric nanomaterial with specific two-dimensional (2D) ferroelectric structures (Figure 2B). The latest report about BMO nanoribbons was proposed by Dong and co-workers, who synthesized BMO nanoribbons via hydrolysis in glycol, and the interplanar spacing referring to the (002) and (062) planes was confirmed through high-resolution transmission electron microscopy (HRTEM).[47] Energy-dispersive spectroscopy (EDS) mapping verified the elements of the synthesized nanomaterials. Interestingly, Dong et al. improved BMO nanoribbons by conjugating them with glutathione (GSH).[47] The GSH-activated BMO (GBMO) nanoribbons were described as featuring better piezoelectricity compared with simple BMO nanoribbons. To measure the generation of ROS caused by the sonodynamic piezocatalytic reaction between BMO/GBMO and US (40 kHz, 3 W cm^{-2}, 50%), such as $\cdot O_2^-$, $_1O_2$, and $\cdot OH$, 1,3-diphenylisobenzofuran (DPBF) and 3,3,5,5-tetramethylbenzidine (TMB) were applied. By measuring the absorbance of DPBF and TMB, it was demonstrated that the GBMO nanoribbons showed increased ROS generation efficiency compared with BMO nanoribbons.

Composite sonosensitizers. Because most organic sonosensitizers are hydrophobic, they are easily cleansed from the blood circulation after intravenous administration, resulting in the decreased accumulation of sonosensitizers at target sites. Thus, efforts have been focused on the modification of sonosensitizers, such as coating sonosensitizers with hydrophilic materials and loading sonosensitizers into nanocarriers to enhance the targeted delivery efficiency. Among the recently explored nanoplatforms, hollow mesoporous organosilicon nanoparticles (HMONs) have been widely employed. Because of their abundant surface area and outstanding biocompatibility, HMONs can be applied to various biomedical applications. For example, Chen et al. loaded the sonosensitizer IR780 into fluorocarbon-chain-decorated HMONs, which can load drugs efficiently and realize stable oxygen delivery.[48] Despite the advantages of inorganic sonosensitizers over organic sonosensitizers, the relatively low production of ROS remains a challenge. Take TiO_2, for instance. The fast recombination of electrons and holes on the surface of a nanostructure leads to a low quantum yield of ROS. Thus, explorations have been made in improving the quantum yield of TiO_2, including noble metal decoration,[49] 2D nanosheet recombination,[50] oxygen-deficient layer attachment,[51] etc.

During the ROS generation process in the interaction between US and sonosensitizers, a large amount of oxygen is consumed, bringing about a limited SDT efficacy. Recent studies have conjugated sonosensitizers to oxygen-generating materials to replenish oxygen during SDT. Numerous nanomaterials such as platinum (Pt) and manganese dioxide (MnO_2) have been reported to generate oxygen through enzyme catalysis.[32,49,52,53] Based on the intrinsic property of Pt, Sun et al. bridged lead and Pt nanocomposites (Pd@Pt) with T790, which is a traditional organic sonosensitizer (Figure 3A).[32] Through covalent conjugation assisted by polyethylene glycol, T790 can be modified with Pd@Pt to form a biocompatible nanocomposite (Pd@Pt-T790). Interestingly, researchers found that the covalent conjugation between Pd@Pt and T790 can be destroyed under US irradiation, thus maintaining the inactive state of Pd@Pt before the nanocomposites reach the targeted site, avoiding unwanted effects. Further studies confirmed that the US-activated oxygen-producing property of Pd@Pt significantly facilitated ROS generation by T790, contributing to the therapeutic efficacy of Pd@Pt-T790. The US-activated catalase activity not only realized the *in situ* generation of oxygen in a brand-new manner, but also paved way for the development of US-triggered nanomotors.

Since sonosensitizers have been explored on the basis of photosensitizers, more and more US-sensitive agents have been analyzed to assist SDT, such as hematoporphyrin and its derivatives,[15] metallic oxide, piezoelectric materials, etc. Although SDT has shown certain antitumor and antibacterial effects based on the generation of ROS, it is still far away from clinical practice. To improve the therapeutic efficacy of SDT, researchers aim at the development of highly efficient sonosensitizers. According to research reported by Wu and co-workers, they fabricated a novel nanocomposite by conjugating gold nanoparticles onto T-BTO (Au@BTO) (Figure 3B).[54] The elemental mapping of the nanocomposites illustrated the distribution of gold nanoparticles on the surface of BTO. Based on the outstanding electromechanical conversion of BTO and the Schottky junction between Au and BTO, a significantly enhanced ROS-generation capacity was elucidated. By measuring the fluorescence spectra of 2-hydroxyterephthalic acid (HTA), which is a reaction product of $\cdot OH$ and terephthalic acid, researchers demonstrated the enhanced $\cdot OH$ generation capacity of US-excited Au@BTO. Moreover, DPBF, which can be degraded by singlet oxygen ($^1O_2$), was applied to measure the US-induced generation of $^1O_2$. The US-activated strong built-in electric field of Au@BTO and the cavitation effect contributed to the significantly improved ROS generation, shedding light on the clinical translation of SDT.

Fluorocarbon compounds

Nowadays, progress in microbubble-based US imaging diagnoses and therapeutic modalities has achieved many successes, but the limited longevity and relatively large volume of the microbubbles prevent them from entering narrower spaces, such as tumor interstitial spaces and some microcapillaries. Researchers have found that the enhanced permeability and retention effects of nanomaterials allow them to locate to targeted sites, contributing to their applications in magnetic resonance imaging (MRI) or computed tomography. However, few nanomaterials can be employed in ultrasonography. Learning from the stable oil emulsions that maintain their character by surfactant coatings, scientists found that nanodroplets with a low boiling point, such as perfluorocarbons (PFCs), may be a feasible regime for ultrasonography. When the liquid PFC is
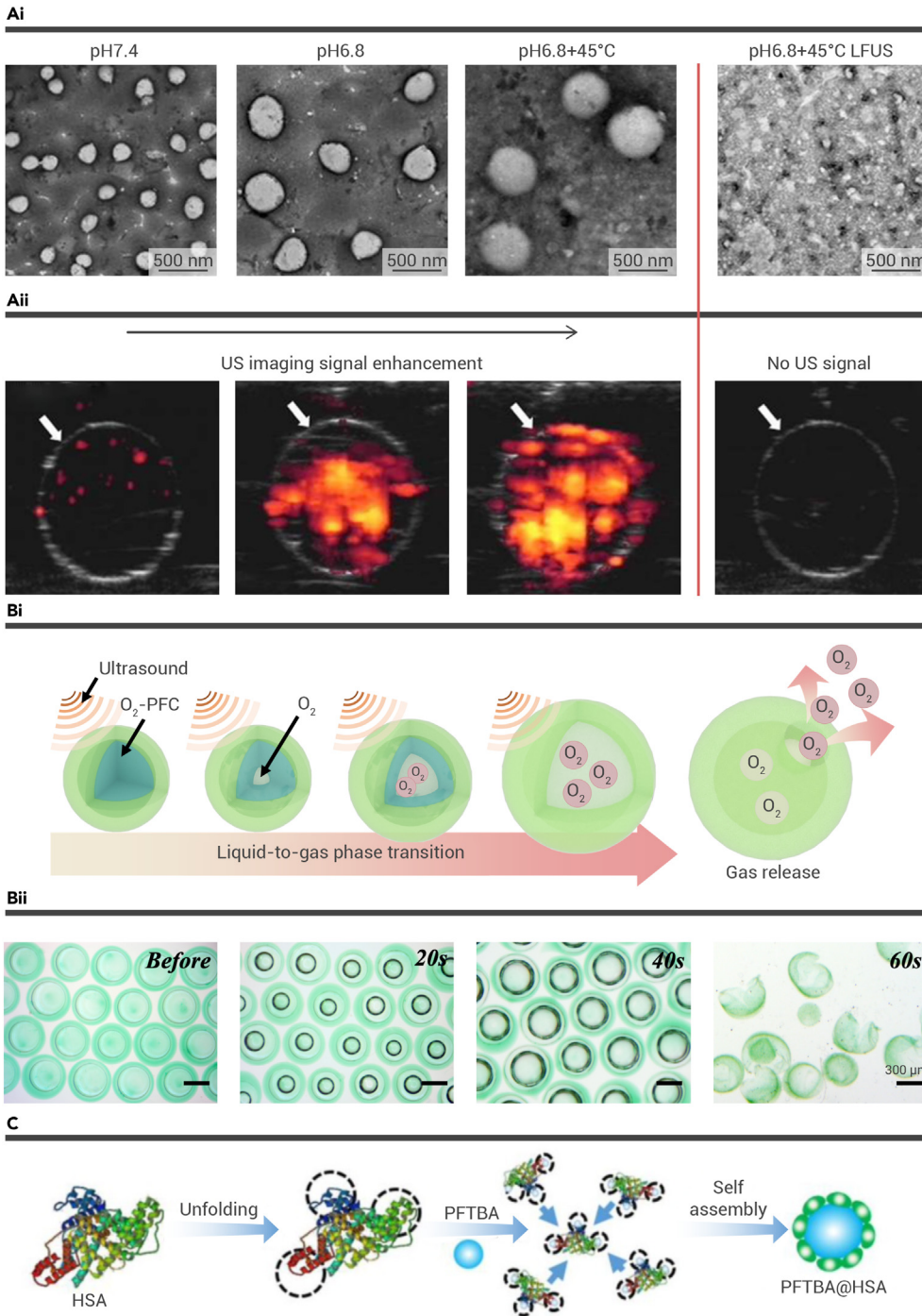
Ai

| pH7.4 | pH6.8 | pH6.8+45°C | pH6.8+45°C LFUS |

500 nm (each of the four panels)

Aii

US imaging signal enhancement → | No US signal

Bi

Ultrasound — O₂-PFC — O₂

Liquid-to-gas phase transition

Gas release

Bii

Before | *20s* | *40s* | *60s*

300 μm

C

HSA → Unfolding → PFTBA → Self assembly → PFTBA@HSA

ing in the clinical diagnosis. Combining the *in situ* phase transition of nanodroplets with therapeutics, it is expected that precise managements of tumors can be achieved. For example, this problem has been addressed by Zhang et al., who proposed PFC-encapsulated theragnostic nanoprobes with a pH-responsive polymer shell (PFP/PFB/doxorubicin [DOX]-PPEHDs) to treat C6 glioma (Figure 4A).[57] The nanoscale of the PFP/PFB/DOX-PPEHDs allowed efficient intratumoral aggregation. The acid microenvironment at the tumor site drove the PFP/PFB/DOX-PPEHDs into larger scale, which would benefit the US-induced phase transition. For the tumors located in deep sites, researchers applied low-frequency US (LFUS) to trigger the liquid-to-gas transition of PFC, bringing about the *in situ* formation of bubbles. The continuous irradiation of LFUS would break the bubbles, thus releasing the loaded DOX at the tumor site. Interestingly, it was demonstrated via power Doppler imaging that the PFP/PFB/DOX-PPEHDs can significantly enhance echogenicity either in agarose phantoms or in *in vivo* tumors, indicating the theragnostic property of these PFC nanoprobes. By encapsulating liquid perfluorohexane (PFH), another kind of PFC, in lipids and cholesterol, nanobubbles can be obtained.[58] As proposed by Shao and co-workers, nanobubbles fabricated with a prepared solution containing drugs can be further conjugated onto the surface of microneedles (MNs) by electrostatic interaction to manufacture nanobubble-loaded MNs.[58] In recent decades, MNs have shown outstanding performance in targeted delivery to multiple parts of the human body, and MNs have been developed to feature distinctive geometries to achieve higher adhesive ability.[59–63] Compared with traditional transdermal drug delivery using drug-loaded MNs, these US-facilitated nanobubble-loaded MNs can achieve a rapid drug penetration and an enhanced agent diffusion, ascribed to microstreaming followed by the cavitation effects of nanobubbles.

Since PFCs were introduced into biomedical applications, they have been employed as a blood substitute, attributed to their biocompatibility and extremely high oxygen solubility, which can reach 20 times that of water. Thus, PFCs are an ideal alternative for delivering oxygen. During SDT for tumors, the interaction between US and sonosensitizers results in a large consumption of oxygen, of which the tumor site is already starved. Tremendous achievements have been made in combining PFCs and SDT to enhance the ROS production of SDT as well as to alleviate the hypoxic microenvironment in tumor sites. Recently, we employed microfluidic electrospray technology to manufacture a microcapsule, the core of which is oxygen-enriched PFCs and the shell of which is a multidrug co-loaded hydrogel (PO/GI-MC) (Figure 4B).[64] Microfluidic technology has emerged as a cutting-edge microscale material fabrication method. Since PFC liquid

supported by a shell, the Laplace pressure provided by the pressures from external environments maintains the PFC in the liquid state. Once the stable PFC is affected by an external stimulus, such as US, the PFC experiences a liquid-to-gas phase transition, during which it can expand five times in volume.[55] Researchers pointed out that this liquid-to-gas phase transition is based on an internal and external cavitation-induced temperature increase.[36,56]

Compared with the microbubbles employed clinically, PFC micro- and nanodroplets can maintain a stable form before reaching the tumor site in the blood circulation. Moreover, like other nanomaterials, nanoscale PFC droplets can reach the tumor interstitial spaces through the enhanced permeability and retention (EPR) effect, which is not hard to realize with bubbles in microscale. Thus, as long as the PFC nanodroplets are targeted to tumors, under the exposure of external US, liquid PFCs undergo the liquid-to-gas phase transition, bringing about *in situ* bubble formation. The bubbles inside the tumor spaces can realize the ultrasonic imaging and represent the tumor shape and size accurately, assist-
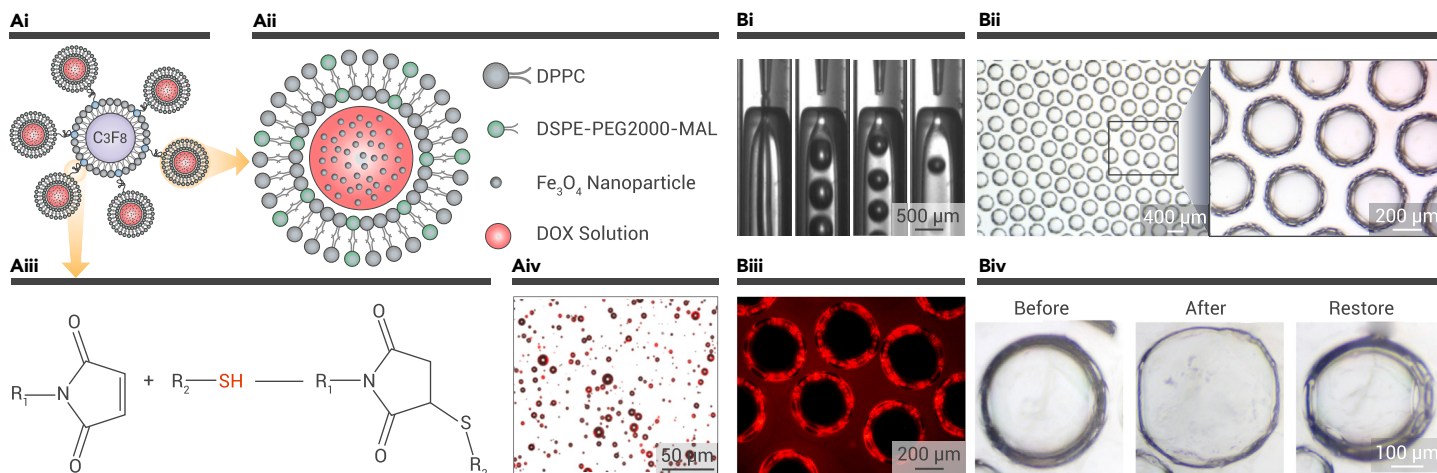
Figure 5. US-responsive lipid and polymer microbubbles (A) Magnetic DOX-ML-MBs. (i−iii) Schematic illustrations of the DOX-ML-MB (i), DOX-loaded magnetic liposomes (ii), and the covalent linkages between liposomes and microbubbles (iii). (iv) Confocal overlay image of DOX-ML-MBs.[80] Copyright 2020, American Chemical Society. (B) US-responsive microfluidic Gem-H$_2$S-UDMs. (i) The microfluidic fabrication process of the microbubbles. (ii) Optical images of the Gem-H$_2$S-UDMs. (iii) Fluorescent dye-loaded microbubbles. (iv) The Gem-H$_2$S-UDM response to the hyperthermia caused by US.[81] Copyright 2021, Wiley-VCH.

features a low boiling point, microfluidic technology allows a moderate fabrication process, thus realizing the maintenance of the physiochemical properties of PFC.[66−74] Ascribed to the US-induced phase-transition ability of PFCs, the PO/GI-MCs experienced the transition from microcapsules to microbubbles when exposed to US waves (1.0 MHz, 1.2 W cm^{-2}). Since the volume of PFCs can become five times larger, the resultant gas core splits the alginate shell, releasing the gas, which contains a large amount of oxygen. By encapsulating the water-soluble chemotherapeutics and sonosensitizers that are sensitive to the same parameters of US in the alginate shell, we realized simultaneous SDT and chemotherapy. Notably, the delivered oxygen enhanced the antitumor efficacy of the chemo-SDT and further alleviated the tumor hypoxia. This multidrug and oxygen co-loaded microcapsule platform exhibited promising potential in US-assisted synergistic antitumor treatment. Moreover, because of the hydrophobicity of PFCs, most of the relevant studies have used lipids to encapsulate PFCs, which seriously limited the loaded drugs. In our study, benefitting from the great maneuverability of microfluidic technology, hydrogel could be applied to fabricate PFC microdroplets, greatly expanding the range of drugs that could be loaded.

In addition to the above-mentioned PFC, perfluorotributylamine (PFTBA), which is another fluorocarbon compound, features more advantages in biomedical application. Studies reported that PFTBA can exert an inhibition effect on platelets, bringing about an enhanced red blood cell (RBC) infiltration at targeted locations.[65] As has been documented, the integrity of tumor vessels is mainly maintained by the active ingredients secreted from platelets.[75] Thus, PFTBA could conceivably exert antitumor efficacy by not only destroying tumor vessels but also delivering oxygen and drugs. Considering the hydrophobic property of the fluorocarbon compound, albumin can be used to encapsulate PFTBA to establish a drug carrier. Another work based on the excellent oxygen delivery properties of PFCs was proposed by Zhou and co-workers, who fabricated two-stage oxygen-delivery nanoparticles using albumin to encapsulate PFTBA (PFTBA@HSA) (Figure 4C).[65] They further demonstrated the excellent oxygen delivery and antiplatelet aggregation properties of PFTBA@HSA. Learning from the excellent features of PFTBA, Huang et al. established an oxygen-carrying nanocarrier (PPID-NPs) to facilitate chemo-SDT.[76] The presented PPID-NP had a polymer shell consisting of poly(lactic-co-glycolic) acid (PLGA), which featured the desired biodegradability and biocompatibility, and a core of PFTBA, which was enriched in oxygen and loaded with sonosensitizer IR780 and DOX. It was demonstrated that under the excitation of US, PPID-NPs showed significantly enhanced drug and oxygen release efficiency. The ROS produced, especially singlet oxygen, from PPID-NPs irradiated by US were significantly higher than those of nanoparticles not containing PFTBA. Furthermore, *in vitro* experiments conducted on 4T1 cells showed that the cells treated with PPID-NPs and US had more intracellular ROS production.

Microbubbles

As widely used US contrast-enhancing agents, microbubbles feature US responsiveness in reflecting harmonic signals upon excitation by US. The tradi-tional agents for CEUS are lipid-shell microbubbles with diameters of approximately 5 μm. Further studies found that, when the US frequency is consistent with the resonance frequency of the microbubbles, the microbubbles will be broken, which is referred to as US-triggered microbubble destruction.[21,77] These two US responses of microbubbles cast light on the innovations of theragnostic microbubbles, which realize not only *in vivo* real-time tracking, but also controllable release of the microbubble-loaded drugs. According to the core-shell structure of microbubbles, researchers focused efforts on feasible and efficient ways to load drugs, such as conjugating drugs onto the shell, encapsulating drugs in the shell, or utilizing therapeutic gas to fill the core. Lipid-shell microbubbles showed excellent *in vivo* CEUS imaging capability.

The stability and longevity of microbubbles *in vivo* are important for effective imaging. To improve the stability of microbubbles and enhance the US signals, Cen and co-workers designed modified PFC-filled microbubbles with amphiphilic fluorinated co-polypeptides.[78] In particular, compared with the commercially applied CEUS agent SonoVue, the fluorinated co-polypeptide-decorated microbubbles showed superior *in vivo* imaging properties. Microbubbles are also promising candidates for drug delivery. Nesbitt et al. proposed lipid microbubbles to deliver the chemotherapeutic gemcitabine and sonosensitizer RB to treat pancreatic cancer through chemo-SDT.[79] The researchers functionalized gemcitabine with biotin and functionalized oxygen-loaded microbubbles (O$_2$MBs) with avidin, followed by attaching the gemcitabine derivatives to the surface of the O$_2$MBs (O$_2$MBs-Gem). Similarly, RB was conjugated to the O$_2$MBs (O$_2$MBs-RB) to apply together with O$_2$MBs-Gem to realize chemo-SDT.

To enhance the targeting ability of the drug-loaded microbubbles, efforts have been made in conjugating target molecules onto microbubbles. In addition, by attaching functional materials that are sensitive to external force fields, such as a magnetic field, enhanced drug accumulation can also be obtained. Recently, Dwivedi's group presented a novel type of microbubble composite, the aggregation of which can be regulated by a magnetic field followed by the activated drug release by external US (Figure 5A).[80] By encapsulating magnetic nanoparticles of Fe$_3$O$_4$ and the chemotherapeutic DOX into liposomes, the obtained magnetic DOX-loaded liposomes can be coupled with microbubbles filled with PFC gas (DOX-ML-MBs). The DOX-ML-MBs display excellent DOX loading efficiency and highly efficient DOX release upon exposure to US. Furthermore, an experiment set up in microfluidic channels illustrated the magnetic activity of the microbubbles. The subsequent animal experiments further elucidated the feasibility of using DOX-ML-MBs along with a magnetic field and US to fight pancreatic cancer.

Although lipid and protein-shell microbubbles have been widely applied in clinical CEUS, the lipophilicity of the shell and limited longevity in the blood circulation severely hamper their drug-loading and delivery capability. To address these problems, polymers have been applied to fabricate microbubbles, such as PLGA, poly(vinyl alcohol), alginate, etc. Compared with the lipid-shell microbubbles, the polymer shell endows the microbubbles with enhanced drug-loading

capacity. In addition, the diverse hydrophilicity or lipophilicity and side chains of the polymer materials improve the selectivity of drugs that can be loaded. For example, hydrophilic drugs can be loaded into a hydrogel shell by being dissolved into the pre-gel solution, and specific peptides can be bound to the side chains of the hydrogel. Zhong et al. applied PLGA to carry a 5-amino-acid peptide through covalent binding.[82] Based on the bond between the peptide and fibrin, these PLGA microbubbles realized the targeted microthrombus detection and thrombus dissolution.

In addition to US-responsive microbubbles activated through the cavitation effect, which release drugs mainly based on the expansion and burst of the gas cores, we designed a kind of polymer-constructed microbubble through a microfluidic electrospray method that is mainly responsive to the thermal effects of US (UDMs) (Figure 5B).[81] The shell of the microbubble was fabricated from a composite hydrogel, which contained the thermosensitive polymer N-isopropylacrylamide (NIPAM) and biocompatible hydrogel alginate. The core of the microbubble was hydrogen sulfide (H_2S), which is a kind of antitumor gas signaling molecule. By encapsulating the water-soluble chemotherapeutic gemcitabine in the hydrogel shell, the polymer microbubble (Gem-H_2S-UDMs) can be implanted into the tumor site to deliver drugs. When US waves (3.0 MHz, 2.0 W cm^{-2}) are applied, the hydrogel shell of the Gem-H_2S-UDMs in the deep tumor site can be triggered to shrink and squeeze out the encapsulated gemcitabine along with water, bringing about the US-triggered *in situ* drug release. Meanwhile, the gas core expands with the increasing temperature, together with the pNIPAM shell thinning from hyperthermic shrinkage, and the H_2S leaks from the core, bringing about the combinational therapy of chemotherapeutics and antitumor gas signaling molecules. Because of the noninvasiveness and permeativity of US, we realized the antitumor treatment in a mouse model of *in situ* deep-sited cancer in a minimally invasive way. Our study provided new ideas for the preparation of US-responsive microbubbles and a way for US-controlled drug release and delivery of gaseous signaling molecules. Moreover, in addition to H_2S, numerous gaseous signaling molecules have been carried by microbubbles and exerted biological effects to achieve therapeutic purposes, such as nitric oxide (NO),[83–85] carbon monoxide,[86–88] etc. For example, Liao's group proposed NO-loaded C4d-targeted microbubbles to successfully treat rats with acute antibody-mediated cardiac allograft rejection due to the immunosuppressive and antithrombotic effects of high NO levels.[83]

However, the polymer microbubbles are defective in *in vivo* imaging due to the relatively limited elasticity compared with lipid microbubbles. Based on the advantages and disadvantages of lipid and polymer microbubbles, Chen and co-workers proposed a novel hybrid microbubble, the shell of which was constructed with lipid and PLGA (Figure 6A).[89] By applying the double-emulsion method and a gas-generating agent, researchers manufactured microbubbles with porous structures, which provided a larger surface and allowed the loading of a large number of drugs. The representative scanning electron microscopy (SEM) image shows the porous structures on the shell. When the lipid/PLGA microbubbles are excited with US (frequency of 5 MHz), strong second signals can be detected at 10 MHz, indicating the stronger CEUS imaging capacity of lipid/PLGA microbubbles. Interestingly, compared with the pure PLGA microbubbles, lipid/PLGA microbubbles had a decreased cavitation threshold. It was demonstrated that the lipid/PLGA microbubbles can be effectively destroyed under specific US waves (frequency of 1 MHz). Thus, by loading DOX into the shell of microbubbles, which was constructed with lipid and PLGA (DOX-lipid/PLGA MBs), a controllable drug release based on the US-mediated microbubble destruction can be achieved (Figure 6B). Thus, the fabricated porous DOX-lipid/PLGA MBs featured not only excellent *in vivo* CEUS imaging capacity but also US-triggered drug release properties. These hybrid microbubbles addressed the limitations of the low drug loading efficiency of lipid-shell microbubbles and the undesired *in vivo* imaging properties of polymer-shell microbubbles, paving the way for the clinical translation of US-responsive multifunctional microbubbles.

Micro- and nanorobots

Nowadays, untethered micro- and nanorobots have attracted tremendous attention in *in vivo* applications such as targeted drug delivery, precision micro/nanosurgery, biopsy and diagnosis of hard-to-reach internal locations, etc. Considerable efforts have been focused on catalytic robots that realize self-propulsion through the chemical substance of surrounding environments, and nowadays external stimulus-propelled robots are required in some chemical

fuel-free circumstances.[90–92] Numerous studies have explored micro- and nanorobots that can be propelled or guided by a magnetic field, electric field, light, US, etc.[93,94] In addition to these broad applied external stimuli, US shows promising potential in navigating microrobots by its biosafety, penetrability, and maneuverability. Because of its controllable navigation and micrometer size, it is feasible to deliver cargo to localized lesion sites. One work worth mentioning is a type of iron oxide nanoparticle containing RBCs as reported by Wu and co-workers (Figure 7A).[95] The fabricated RBC motor could be navigated by external US and a magnetic field, which was ascribed to the uneven distribution of the iron oxide nanoparticles within RBCs that feature asymmetric morphology. In another research reported by de Ávila et al., a dual-cell membrane-coated gold nanowire (RBC-PL robot) was designed for US-guided pathogen targeting and neutralization (Figure 7B).[96] The RBC membrane and platelet membrane endowed the nanorobots with various biological advantages, such as bacteria adhesion and toxin neutralization.

Based on the cavitation effect, which demonstrates US-activated bubble generation and the resonant oscillation of these bubbles, researchers have explored the interaction between the bubble size and the activating resonance frequencies. Thus, it is anticipated that microbubbles could be utilized as the power engine for US-activated microrobots. As reported by Liu and Cho, a US-activated bubble-propelled 3D microdrone was designed by assembling gas-trapped one-end-open microtubes with different lengths and directions (Figure 8A).[97] Since the bubbles with different sizes respond only to a specific acoustic resonance frequency, the 3D microdrone can be remotely navigated in various directions by US with different frequencies.

Recently, Aghakhani and co-workers addressed the limitation that most of the microrobots were able to propel only in homogeneous Newtonian fluids, and they designed acoustic microrobots that could be propelled in complex biological fluids (Figure 8B).[98] Similarly, this microrobot featured a hollow body, which contained an oscillatory microbubble. Under the excitation of US with a specific frequency, the microbubble-trapped microrobot generated a strong microstream, which served as propulsion for the movement of the microrobot. Interestingly, the double reentrant edge designed inside the hollow body of the microrobot contributed to a strong liquid repellency at the interface of liquid and gas, thus enabling the stability of the microbubbles in different fluids. Furthermore, researchers explored the differentiation between Janus magnetic microrobots activated by a rotational uniform magnetic field and an acoustic microrobot activated by US. In contrast to the homogeneous Newtonian fluids, non-Newtonian fluids, such as mucus, feature a viscoelastic nature that would provide a resistive force when microrobots are propelled by a magnetic field, leading to the pushing back of the Janus magnetic microrobots. However, the mutual effects between the disrupted microstream and the thrust force inside the non-Newtonian fluid could effectively actuate the microrobots, contributing to the propulsion of the acoustic microrobot in the mucus medium. These advancements presented by Aghakhani et al. did pave the way for the biomedical application and clinical translation of US-activated microrobots.

CONCLUSION AND OUTLOOK

Recent advances in the discovery of US mechanisms and distinctive engineering of US-responsive matters have shown the promising practical significance of US. In this review, we have demonstrated typical and recent developments of US-responsive matters and their biomedical values. From the diagnostic aspect, US-responsive microbubbles and nanodroplets can reach deep-seated locations and feed back information on lesions. By modifying these platforms with functional groups, the microbubbles and nanodroplets can realize multimode imaging and synergistic treatment. The studies on nanoscale materials led to the biosensing application of US, from detecting endogenous molecules to sensing microenvironments. For therapeutic applications, US can exert therapeutic effects from two aspects: one is through the US-mediated physiochemical effects, another is through US-triggered payload release and activation. SDT is based on US-induced ROS generation, which occurs via acoustic energy conversion and other ways. HIFU ablation and sonothermal therapy are ascribed to the thermal effects resulting from cavitation effects, interactions between US and tissues, and so on. US-mediated thrombolysis is based on microbubble-facilitated cavitation effects. In contrast, the deep penetrability and efficient energy transfer of US realize navigated drug delivery and the release of targeted drugs, including chemotherapeutics, gases, genes, proteins, engineered bacteria, etc. These
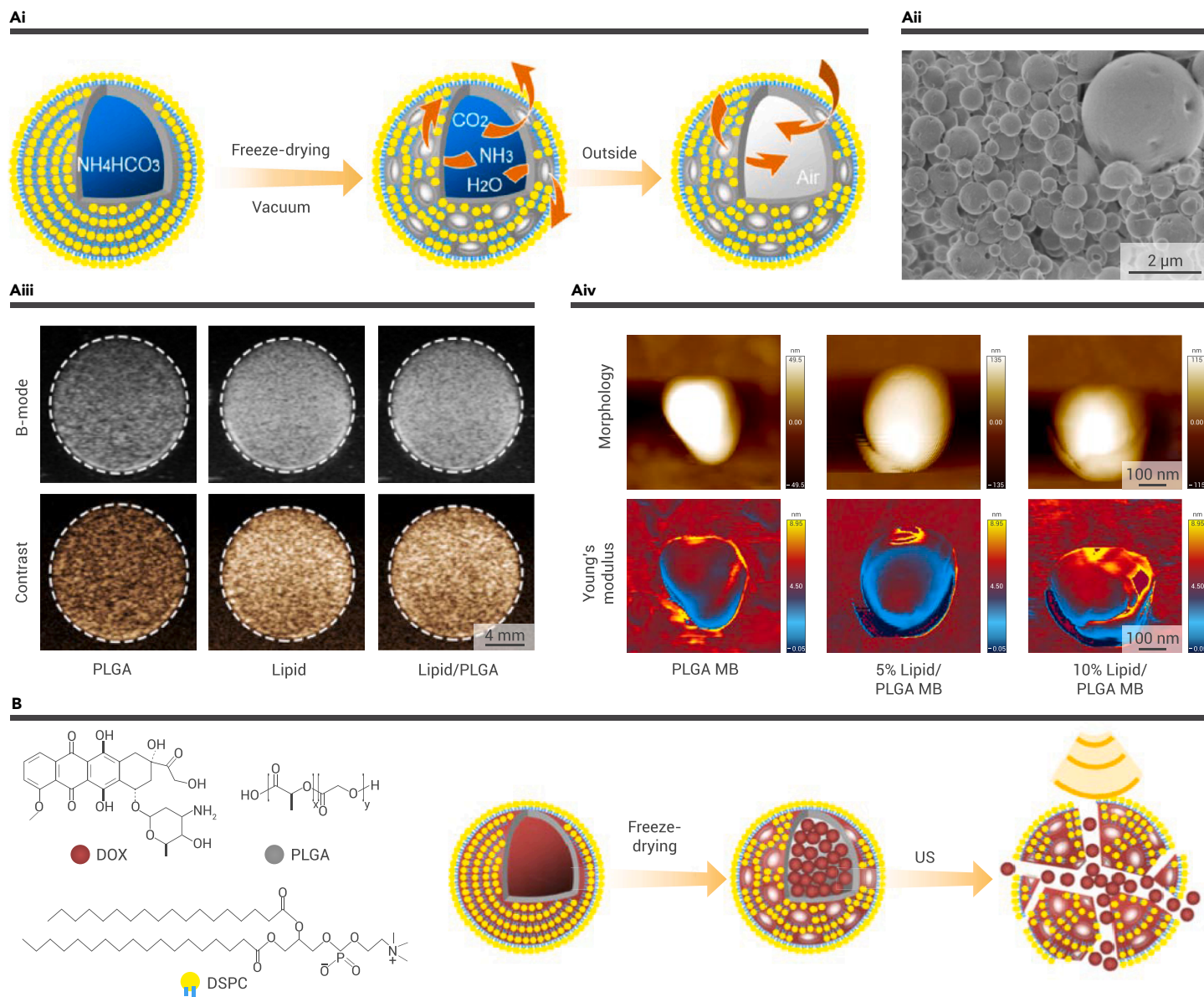
Ai

Aii

Aiii

Aiv

B

Figure 6. US-responsive hybrid microbubbles (A) Fabrication and characterization of lipid/PLGA MBs. (i) Schematic diagram of the fabrication process of lipid/PLGA MBs. (ii) SEM image showing the porous structures on the shell. (iii) Ultrasonographs of PLGA MBs, lipid MBs, and lipid/PLGA MBs. (iv) Young's modulus results for lipid/PLGA MBs with diverse lipid ratios showing the softened shell of lipid/PLGA MBs. (B) Schematic diagram of the fabrication process and drug-release property of DOX-lipid/PLGA MBs.[89] Copyright 2019, American Chemical Society.

thrilling achievements have greatly expanded the use of US in multidisciplinary fields, while many aspects remain to be further optimized and refined to make US more practical.

For decades, US and diverse US contrast agents have been applied clinically with remarkable diagnostic effects. The earliest US contrast agents were microbubbles containing carbon dioxide, oxygen, or air. These microbubbles were mainly produced by hand shaking of normal saline, which could be used only for simple heart system imaging. Then, to extend the microbubbles' stability and longevity for prolonged observing time and internal retention time, researchers used more stable and safer materials to wrap the gas around, such as denatured albumin, liposomes, polymers, and various surfactants. To date, many US contrast-enhancing agents have been commercially produced and widely employed in clinical applications, contributing considerably to the identification and differentiation of diseases; examples are SonoVue and Sonazoid. Although these contrast agents are easy to store and transport and are widely used in clinical practice, they still have some disadvantages in short imaging and observing time, hindering the long-time scanning of larger organs and repeated observation of target lesions. On the other hand, the materials used in fabricating microbubbles might have some allergenicity. Sonazoid, for

example, although it can be used for specific Kupffer cell imaging, it cannot be used in patients with egg allergy due to its shell component containing sodium hydrolecithin serine. At the same time, nanobubbles and nanospheres are the development trend of multifunctional contrast agents due to the limited depth of microscale bubbles in exploring tissues. Therefore, the cooperation of multiple disciplines is highly required to develop and synthesize more biocompatible and multifunctional materials for microbubble preparation.

The various parameters of frequency and power of US waves can greatly affect its application. Cavitation bubbles will vibrate under the action of an ultrasonic field. When the frequency of ultrasonic waves is less than the vibration frequency of cavitation bubbles, the cavitation bubbles will collapse. The resonance frequency of the microbubble is related to many factors, such as the diameter of the microbubble, the density of the liquid around the microbubble, and the room temperature and pressure outside the microbubble. Therefore, the development of flexible and controllable instruments to fabricate microbubbles with regulable diameters and compositions is an important link to promote the development of multifunctional microbubbles.

On the other hand, the development of an accurate and portable machine capable of generating ultrasonic waves of various frequencies and powers is of
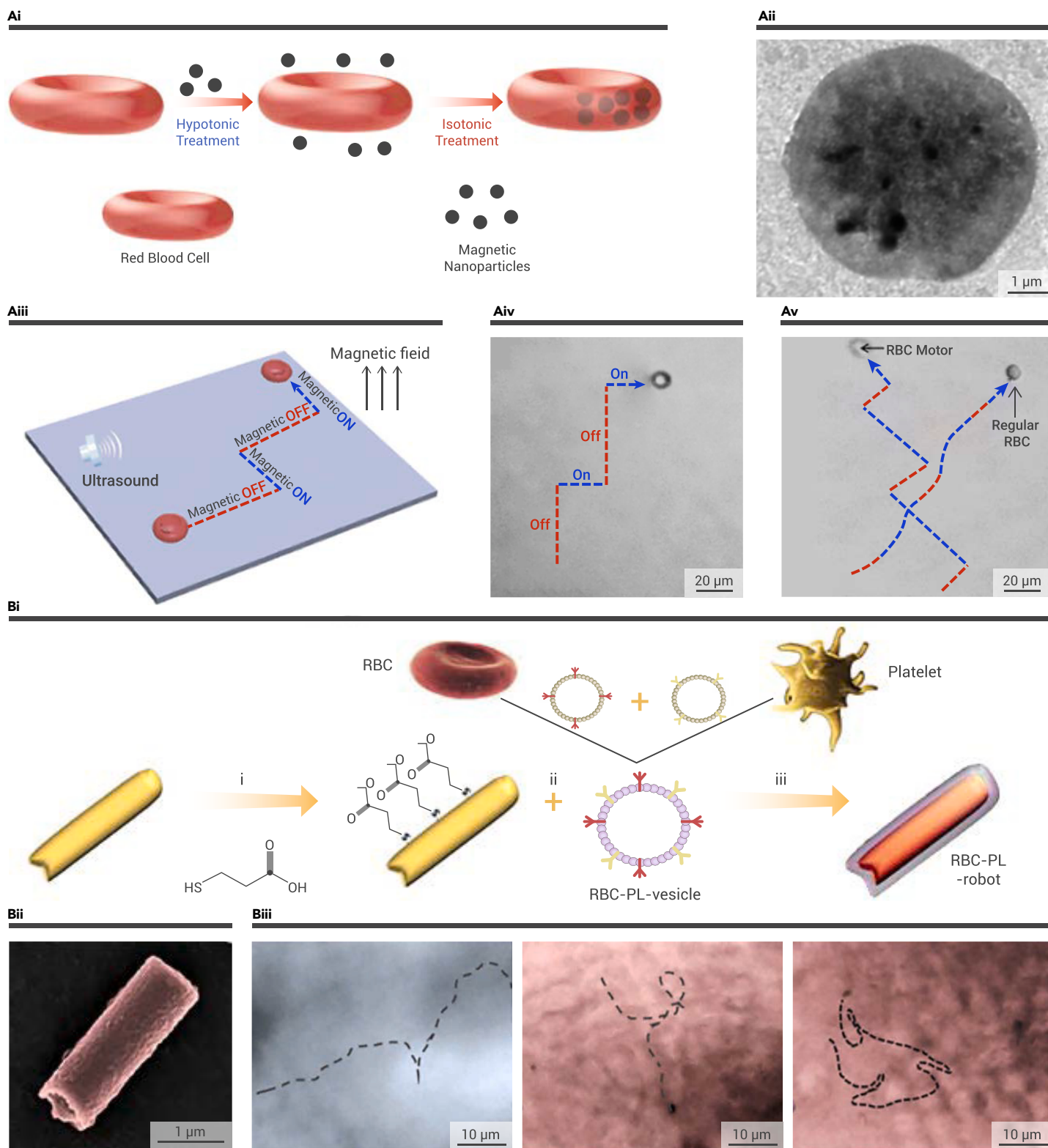
Figure 7. US-propelled micro- and nanorobots (A) Magnetic nanoparticle-loaded RBC motors. (i) Scheme of the fabrication process and (ii) TEM image of the RBC motors. (iii) Scheme of the magneto-switchable guidance of the RBC motors. (iv) Real-time images of the movement of a magnetic nanoparticle-loaded RBC motor and (v) in presence of a natural RBC.[95] Copyright 2014, American Chemical Society. (B) US-guided pathogen-targeting RBC-PL robot. (i) Schemes of the US-powered nanorobots for bacterium adhesion and toxin neutralizations. (ii) SEM image of an RBC-PL robot. (iii) The tracking trajectories of the RBC-PL robot in water and in blood.[96] Copyright 2018, the authors.

great value for the promotion and application of US-responsive materials. Generally, some hospitals have rehabilitation departments equipped with US therapy instruments, which can output US waves with specific powers and frequencies and are equipped with probes of different sizes for different body parts. Although these US therapy instruments can be used at the bedside and are very portable, making them very convenient for clinical use, their ability to adjust ultrasonic parameters is limited. Compared with professional acoustic instruments, US therapy instruments are unable to produce US waves with fine-tuned parameters. However, the operation of professional acoustic instruments is complex and bulky, which is not conducive to the clinical application of ultrasonic-responsive materials. Typically, different sonosensitizers respond only to US with different specific frequencies and powers. Under the excitation of US with a specific frequency and
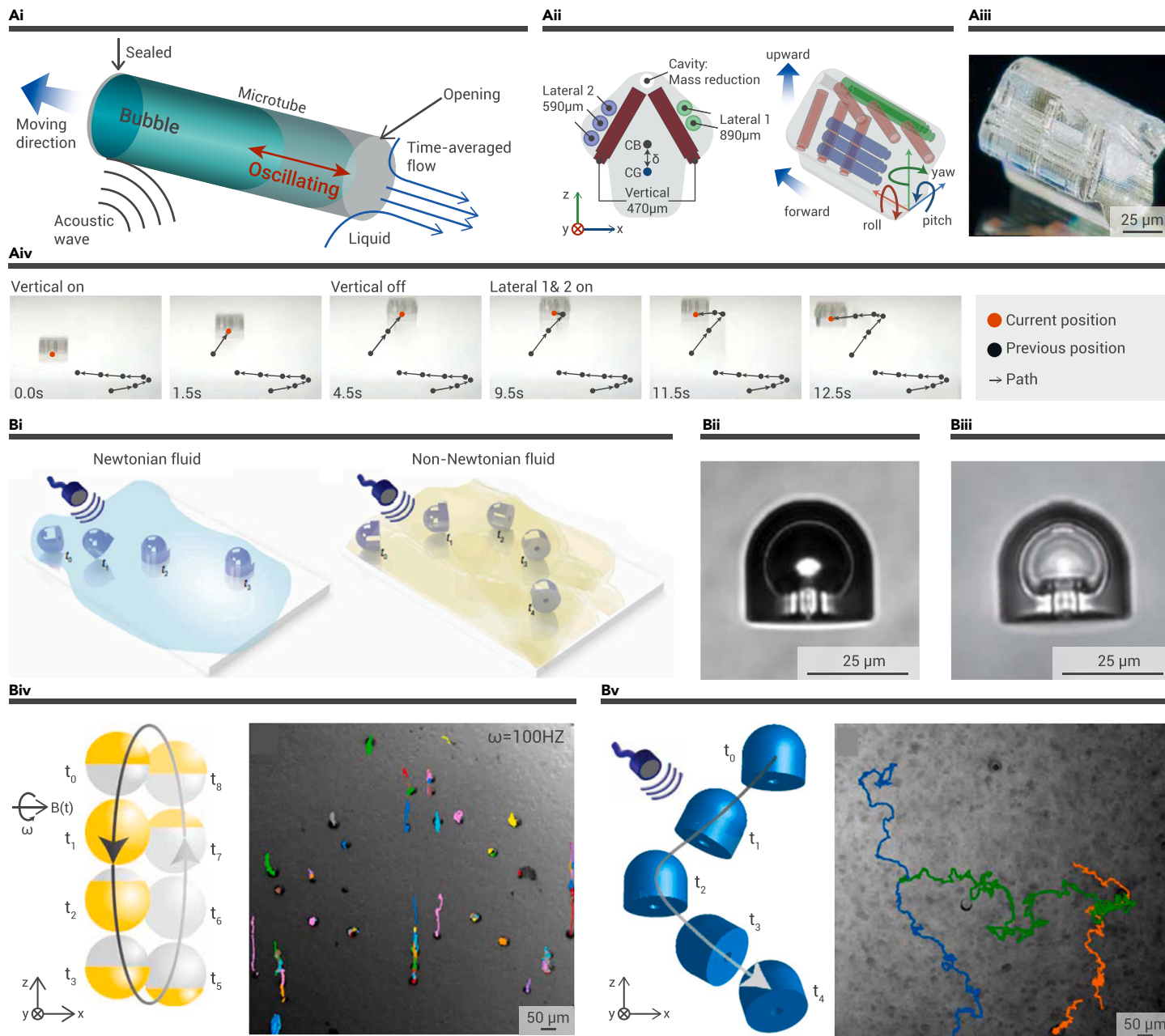
Figure 8. US-responsive microbubble-activated microrobots (A) US-activated bubble-propelled 3D microdrone. (i) Schematic illustration of the mechanism of US-activated oscillating gaseous bubble for propelling the microdrone. (ii) Schematic design showing the three groups of microtubes in the microdrone. (iii) Digital image of the microdrone. (iv) Tracking trajectories showed the US controllability and repeatability of the 3D microdrone.[97] Copyright 2020, The Royal Society of Chemistry. (B) The 3D-printed acoustic microrobots. (i) Schemes of the microrobots in Newtonian and non-Newtonian fluid. (ii) A microrobot encasing a microbubble in PBS. (iii) A microrobot filled with low-surface-tension liquid. (iv and v) Comparison of the under-mucus motion between magnetic microrobots (iv) and acoustic microrobots (v).[98] Copyright 2022, the authors.

power, sonosensitizers show better ROS generation properties, contributing to the therapeutic efficacy. For example, studies found that ICG is more sensitive to US at 1 MHz, 1.61 W cm^{-2},[99] IR780 is more sensitive to US at 650 kHz, 2.4 W cm^{-2},[100] TiO$_2$ is more sensitive to US at 0.8 MHz, 1.5 W cm^{-2},[101] etc. Therefore, future efforts could be focused on the development of smart US transducers and new sonosensitizers for highly efficient ROS production. Moreover, the exploration of the optimal US parameters to excite the US-responsive materials is also significant. Since US-triggered therapeutic modalities are still under experimental research and clinical trials, a definite guideline for the employment of US parameters is still lacking. However, some authoritative reviews have summarized the acoustic properties and optimal US parameters of various materials in detail, which is worthy of reference and learning.[1,20,102,103]

All the research and exploration of the above-mentioned US-responsive matters are ultimately for the purpose of contributing to human health. The practical application of US-responsive matters is inseparable from clinical experiments and the cooperation and promotion of clinicians. Numerous US-based clinical studies are also underway, some of which have yielded promising results. Meanwhile, in addition to HIFU and SDT, scientists and physicians have discovered the therapeutic and adjunctive role of US in more and more treatments. Although the mechanisms between US and the US-responsive matters are still far from complete, the practical feasibility is positive, and more detailed information about the US mechanisms is being discovered. The safety concerns of US and US-responsive matters are also great challenges that require attention before wide clinical application. With the addressing of current problems and innovation of more US-responsive matters, the application of US can be further expanded to much wider fields.

REFERENCES

1. Athanassiadis, A.G., Ma, Z., Moreno-Gomez, N., et al. (2022). Ultrasound-responsive systems as components for smart materials. Chem. Rev. **122**, 5165–5208.

2. Böhm, M., and Lauder, L. (2021). Blood pressure and renal denervation with ultrasound: another step forward. Lancet **397**, 2441−2443.

3. Waksman, R., Di Mario, C., Torguson, R., et al. (2019). Identification of patients and plaques vulnerable to future coronary events with near-infrared spectroscopy intravascular ultrasound imaging: a prospective, cohort study. Lancet **394**, 1629−1637.

4. Küng, E., Habrina, L., Berger, A., et al. (2021). Diagnosing pneumomediastinum in a neonate using a lung ultrasound. Lancet **398**, e13.

5. Allocca, M., Kucharzik, T., and Rubin, D.T. (2023). Intestinal ultrasound in the assessment and management of inflammatory bowel disease: is it ready for standard practice? Gastroenterology.

6. Seneviratne, N., Fang, C., and Sidhu, P.S. (2023). Ultrasound-based hepatic fat quantification: current status and future directions. Clin. Radiol. **78**, 187−200.

7. Erlinge, D., Maehara, A., Ben-Yehuda, O., et al. (2021). Identification of vulnerable plaques and patients by intracoronary near-infrared spectroscopy and ultrasound (PROSPECT II): a prospective natural history study. Lancet **397**, 985−995.

8. Diao, X., Zhan, J., Chen, L., et al. (2020). Role of superb microvascular imaging in differentiating between malignant and benign solid breast masses. Clin. Breast Cancer **20**, e786−e793.

9. Danqing, H.M., Min, T.M., Aimei, L.M., et al. (2022). Neurofibromatosis with intrahepatic, retroperitoneal and pelvic involvement: a case report and literature review. Adv. ULTRASOUND DIAGNOSIS Ther. **6**, 29.

10. Yu, Y., Ye, X., Yang, J., et al. (2022). Application of a shear-wave elastography prediction model to distinguish between benign and malignant breast lesions and the adjustment of ultrasound Breast Imaging Reporting and Data System classifications. Clin. Radiol. **77**, e147−e153.

11. Chen, Y., Mao, R., Xie, X., et al. (2016). Intracavitary contrast-enhanced ultrasonography to detect enterovesical fistula in crohn's disease. Gastroenterology **150**, 315−317.

12. Kong, W.T., Wang, W.P., Shen, H.Y., et al. (2021). Hepatic inflammatory pseudotumor mimicking malignancy: the value of differential diagnosis on contrast enhanced ultrasound. Med. Ultrason. **23**, 15−21.

13. Dietrich, C.F., Nolsøe, C.P., Barr, R.G., et al. (2020). Guidelines and good clinical practice recommendations for contrast enhanced ultrasound (CEUS) in the liver − update 2020 − WFUMB in cooperation with EFSUMB, AFSUMB, AIUM, and FLAUS. Ultraschall der Medizin - Eur. J. Ultrasound.Ultraschall Med. **41**, 562−585.

14. Kong, W.T., Shen, H.Y., Qiu, Y.D., et al. (2018). Application of contrast enhanced ultrasound in gallbladder lesion: is it helpful to improve the diagnostic capabilities? Med. Ultrason. **20**, 420−426.

15. Yumita, N., Nishigaki, R., Umemura, K., et al. (1989). Hematoporphyrin as a sensitizer of cell-damaging effect of ultrasound. Japanese J. Cancer Res. **80**, 219−222.

16. Yao, J., Gao, W., Wang, Y., et al. (2020). Sonodynamic therapy suppresses neovascularization in atherosclerotic plaques via macrophage apoptosis-induced endothelial cell apoptosis. JACC Basic to Transl. Sci. **5**, 53−65.

17. Dimcevski, G., Kotopoulis, S., Bjånes, T., et al. (2016). A human clinical trial using ultrasound and microbubbles to enhance gemcitabine treatment of inoperable pancreatic cancer. J. Contr. Release **243**, 172−181.

18. Lin, X., Song, J., Chen, X., et al. (2020). Ultrasound-activated sensitizers and applications. Angew. Chem., Int. Ed. Engl. **59**, 14212−14233.

19. Umemura, S., Yumita, N., Nishigaki, R., et al. (1990). Mechanism of cell damage by ultrasound in combination with hematoporphyrin. Jpn. J. Cancer Res. **81**, 962−966.

20. Son, S., Kim, J.H., Wang, X., et al. (2020). Multifunctional sonosensitizers in sonodynamic cancer therapy. Chem. Soc. Rev. **49**, 3244−3261.

21. Li, Y., Chen, Z., and Ge, S. (2021). Sonoporation: underlying mechanisms and applications in cellular regulation. BIO Integr **2**, 29−36.

22. Feril, L.B., and Tachibana, K. (2012). Use of ultrasound in drug delivery systems: emphasis on experimental methodology and mechanisms. Int. J. Hyperther. **28**, 282−289.

23. Hersh, D.S., and Eisenberg, H.M. (2018). Current and future uses of transcranial focused ultrasound in neurosurgery. J. Neurosurg. Sci. **62**, 203−213.

24. Wang, Y., Wang, W., Xu, H., et al. (2017). Non-lethal sonodynamic therapy inhibits atherosclerotic plaque progression in ApoE-/- mice and attenuates ox-LDL-mediated macrophage impairment by inducing Heme Oxygenase-1. Cell. Physiol. Biochem. **41**, 2432−2446.

25. Coussios, C.C., and Roy, R.A. (2008). Applications of acoustics and cavitation to noninvasive therapy and drug delivery. Annu. Rev. Fluid Mech. **40**, 395−420.

26. Liang, C., Xie, J., Luo, S., et al. (2021). A highly potent ruthenium(II)-sonosensitizer and sonocatalyst for in vivo sonotherapy. Nat. Commun. **12**, 5001.

27. Gao, D., Xu, M., Cao, Z., et al. (2015). Ultrasound-triggered phase-transition cationic nanodroplets for enhanced gene delivery. ACS Appl. Mater. Interfaces. **7**, 13524−13537.

28. Lyon, P.C., Gray, M.D., Mannaris, C., et al. (2018). Safety and feasibility of ultrasound-triggered targeted drug delivery of doxorubicin from thermosensitive liposomes in liver tumours (TARDOX): a single-centre, open-label, phase 1 trial. Lancet Oncol. **19**, 1027−1039.

29. Curley, C.T., Mead, B.P., Negron, K., et al. (2020). Augmentation of brain tumor interstitial flow via focused ultrasound promotes brain-penetrating nanoparticle dispersion and transfection. Sci. Adv. **6**, eaay1344.

30. Sloand, J.N., Nguyen, T.T., Zinck, S.A., et al. (2020). Ultrasound-guided cytosolic protein delivery via transient fluorous masks. ACS Nano **14**, 4061−4073.

31. Huo, S., Zhao, P., Shi, Z., et al. (2021). Mechanochemical bond scission for the activation of drugs. Nat. Chem. **13**, 131−139.

32. Sun, D., Pang, X., Cheng, Y., et al. (2020). Ultrasound-switchable nanozyme augments sonodynamic therapy against multidrug-resistant bacterial infection. ACS Nano **14**, 2063−2076.

33. Costley, D., Mc Ewan, C., Fowley, C., et al. (2015). Treating cancer with sonodynamic therapy: a review. Int. J. Hyperther. **31**, 107−117.

34. Rengeng, L., Qianyu, Z., Yuehong, L., et al. (2017). Sonodynamic therapy, a treatment developing from photodynamic therapy. Photodiagnosis Photodyn. Ther. **19**, 159−166.

35. Wang, H., Guo, Y., Wang, C., et al. (2021). Light-controlled oxygen production and collection for sustainable photodynamic therapy in tumor hypoxia. Biomaterials **269**, 120621.

36. Giesecke, T., and Hynynen, K. (2003). Ultrasound-mediated cavitation thresholds of liquid perfluorocarbon droplets in vitro. Ultrasound Med. Biol. **29**, 1359−1365.

37. Everbach, E.C., and Francis, C.W. (2000). Cavitational mechanisms in ultrasound-accelerated thrombolysis at 1 MHz. Ultrasound Med. Biol. **26**, 1153−1160.

38. Tang, Q., Chang, S., Tian, Z., et al. (2017). Efficacy of indocyanine green-mediated sonodynamic therapy on rheumatoid arthritis fibroblast-like synoviocytes. Ultrasound Med. Biol. **43**, 2690−2698.

39. Li, W., Song, Y., Liang, X., et al. (2021). Mutual-reinforcing sonodynamic therapy against rheumatoid arthritis based on sparfloxacin sonosensitizer doped concave-cubic rhodium nanozyme. Biomaterials **276**, 121063.

40. Gupta, S.C., Patchva, S., and Aggarwal, B.B. (2013). Therapeutic roles of curcumin: lessons learned from clinical trials. AAPS J. **15**, 195−218.

41. Zheng, L., Sun, X., Zhu, X., et al. (2014). Apoptosis of THP-1 derived macrophages induced by sonodynamic therapy using a new sonosensitizer hydroxyl acetylated curcumin. PLoS One **9**, e93133.

42. Wang, J., Jiao, Y., and Shao, Y. (2018). Mesoporous silica nanoparticles for dual-mode chemo-sonodynamic therapy by low-energy ultrasound. Materials **11**, 2041.

43. Li, C., Yang, X.-Q., An, J., et al. (2020). Red blood cell membrane-enveloped O 2 self-supplementing biomimetic nanoparticles for tumor imaging-guided enhanced sonodynamic therapy. Theranostics **10**, 867−879.

44. Gao, F., He, G., Yin, H., et al. (2019). Titania-coated 2D gold nanoplates as nanoagents for synergistic photothermal/sonodynamic therapy in the second near-infrared window. Nanoscale **11**, 2374−2384.

45. Deepagan, V.G., You, D.G., Um, W., et al. (2016). Long-circulating Au-TiO 2 nanocomposite as a sonosensitizer for ROS-mediated eradication of cancer. Nano Lett. **16**, 6257−6264.

46. Zhu, P., Chen, Y., and Shi, J. (2020). Piezocatalytic tumor therapy by ultrasound-triggered and BaTiO 3 -mediated piezoelectricity. Adv. Mater. **32**, 2001976.

47. Dong, Y., Dong, S., Liu, B., et al. (2021). 2D piezoelectric Bi 2 MoO 6 nanoribbons for GSH-enhanced sonodynamic therapy. Adv. Mater. **33**, 2106838.

48. Chen, J., Luo, H., Liu, Y., et al. (2017). Oxygen-self-produced nanoplatform for relieving hypoxia and breaking resistance to sonodynamic treatment of pancreatic cancer. ACS Nano **11**, 12849−12862.

49. Liang, S., Deng, X., Xu, G., et al. (2020). A novel Pt−TiO 2 heterostructure with oxygen-deficient ILayer as bilaterally enhanced sonosensitizer for synergistic chemo-sonodynamic cancer therapy. Adv. Funct. Mater. **30**, 1908598.

50. Dai, C., Zhang, S., Liu, Z., et al. (2017). Two-dimensional graphene augments nanosonosensitized sonocatalytic tumor eradication. ACS Nano **11**, 9467−9480.

51. Han, X., Huang, J., Jing, X., et al. (2018). Oxygen-deficient black titania for synergistic/enhanced sonodynamic and photoinduced cancer therapy at near infrared-II biowindow. ACS Nano **12**, 4545−4555.

52. Lin, H., Chen, Y., and Shi, J. (2018). Nanoparticle-triggered in situ catalytic chemical reactions for tumour-specific therapy. Chem. Soc. Rev. **47**, 1938−1958.

53. Wang, D., Wu, H., Lim, W.Q., et al. (2019). A mesoporous nanoenzyme derived from metal−organic frameworks with endogenous oxygen generation to alleviate tumor hypoxia for significantly enhanced photodynamic therapy. Adv. Mater. **31**, 1901893.

54. Wu, M., Zhang, Z., Liu, Z., et al. (2021). Piezoelectric nanocomposites for sonodynamic bacterial elimination and wound healing. Nano Today **37**, 101104.

55. Lea-Banks, H., O'Reilly, M.A., and Hynynen, K. (2019). Ultrasound-responsive droplets for therapy: a review. J. Contr. Release **293**, 144−154.

56. Schad, K.C., and Hynynen, K. (2010). In vitro characterization of perfluorocarbon droplets for focused ultrasound therapy. Phys. Med. Biol. **55**, 4933−4947.

57. Zhang, L., Yin, T., Li, B., et al. (2018). Size-modulable nanoprobe for high-performance ultrasound imaging and drug delivery against cancer. ACS Nano **12**, 3449−3460.

58. Shao, S., Wang, S., Ren, L., et al. (2022). Layer-by-layer assembly of lipid nanobubbles on microneedles for ultrasound-assisted transdermal drug delivery. ACS Appl. Bio Mater. **5**, 562−569.

59. Sanjay, S.T., Zhou, W., Dou, M., et al. (2018). Recent advances of controlled drug delivery using microfluidic platforms. Adv. Drug Deliv. Rev. **128**, 3−28.

60. Zhang, X., Wang, F., Yu, Y., et al. (2019). Bio-inspired clamping microneedle arrays from flexible ferrofluid-configured moldings. Sci. Bull. **64**, 1110−1117.

61. Fu, X., Zhang, X., Huang, D., et al. (2022). Bioinspired adhesive microneedle patch with gemcitabine encapsulation for pancreatic cancer treatment. Chem. Eng. J. **431**, 133362.

62. Zhang, X., Chen, G., Cai, L., et al. (2022). Dip-printed microneedle motors for oral macromolecule delivery. Research **2022**, 9797482.

63. Huang, D., Fu, X., Zhang, X., et al. (2022). Christmas tree-shaped microneedles as FOLFIRINOX spatiotemporal delivery system for pancreatic cancer treatment (Research), p. 2022.

64. Huang, D., Zhao, C., Wen, B., et al. (2022). Oxygen-carrying microfluidic microcapsules for enhancing chemo-sonodynamic therapy on patient-derived tumor organoid models. Chem. Eng. J. **435**, 134871.

65. Zhou, Z., Zhang, B., Wang, H., et al. (2018). Two-stage oxygen delivery for enhanced radiotherapy by perfluorocarbon nanoparticles. Theranostics **8**, 4898−4911.

66. Guo, J., Yu, Y., Zhang, D., et al. (2021). Morphological hydrogel microfibers with MXene encapsulation for electronic skin. Research **2021**, 7065907−7065910.

67. Huang, D., Zhang, X., Fu, X., et al. (2021). Liver spheroids on chips as emerging platforms for drug screening. Eng. Regen. **2**, 246−256.

68. Wang, J., Huang, D., Yu, H., et al. (2022). Biohybrid response microparticles decorated with trained-MSCs for acute liver failure recovery. Adv. Healthc. Mater. **11**, 2201085.

69. Wang, J., Huang, D., Ren, H., et al. (2022). Biomimic trained immunity-MSCs delivery microcarriers for acute liver failure regeneration. Small **18**, 2200858.

70. Luo, Z., Che, J., Sun, L., et al. (2021). Microfluidic electrospray photo-crosslinkable κ-Carrageenan microparticles for wound healing. Eng. Regen. **2**, 257−262.

71. Zhuge, W., Liu, H., Wang, W., et al. (2022). Microfluidic bioscaffolds for regenerative engineering. Eng. Regen. **3**, 110−120.

72. Zhang, D., Li, W., Shang, Y., et al. (2022). Programmable microfluidic manipulations for biomedical applications. Eng. Regen. **3**, 258−261.

73. Gao, Y., and Ma, Q. (2022). Bacterial infection microenvironment-responsive porous microspheres by microfluidics for promoting anti-infective therapy. Smart Med **1**.

74. Chen, H., Guo, J., Bian, F., et al. (2022). Microfluidic technologies for cell deformability cytometry. Smart Med **1**.

75. Pidcoke, H.F., Shade, R.E., Herzig, M.C., et al. (2013). A third generation perfluorocarbon causes thrombocytopenia, platelet dysfunction and changes in blood morphology in a baboon model of systemic inflammation. Blood **122**, 2327.

76. Huang, B., Chen, S., Pei, W., et al. (2020). Oxygen-sufficient nanoplatform for chemo-sonodynamic therapy of hypoxic tumors. Front. Chem. **8**, 358.

77. Zhang, C., Chen, S., Li, Q., et al. (2021). Ultrasound-targeted microbubble destruction mediates gene transfection for Beta-cell regeneration and glucose regulation. Small **17**, 2008177.

78. Cen, J., Ye, X., Liu, X., et al. (2022). Fluorinated copolypeptide-stabilized microbubbles with maleimide-decorated surfaces as long-term ultrasound contrast agents. Angew. Chem., Int. Ed. Engl. **61**, e202209610.

79. Nesbitt, H., Sheng, Y., Kamila, S., et al. (2018). Gemcitabine loaded microbubbles for targeted chemo-sonodynamic therapy of pancreatic cancer. J. Contr. Release **279**, 8−16.

80. Dwivedi, P., Kiran, S., Han, S., et al. (2020). Magnetic targeting and ultrasound activation of liposome−microbubble conjugate for enhanced delivery of anticancer therapies. ACS Appl. Mater. Interfaces. **12**, 23737−23751.

81. Huang, D., Zhang, X., Zhao, C., et al. (2021). Ultrasound-responsive microfluidic microbubbles for combination tumor treatment. Adv. Ther. **4**, 2100050.

82. Zhong, Y., Zhang, Y., Xu, J., et al. (2019). Low-intensity focused ultrasound-responsive phase-transitional nanoparticles for thrombolysis without vascular damage: a synergistic nonpharmaceutical strategy. ACS Nano **13**, 3387−3403.

83. Liao, T., Li, Q., Zhang, Y., et al. (2020). Precise treatment of acute antibody-mediated cardiac allograft rejection in rats using C4d-targeted microbubbles loaded with nitric oxide. J. Heart Lung Transplant. **39**, 481−490.

84. Shekhar, H., Palaniappan, A., McDaniel, C., et al. (2018). Characterization of lipid-encapsulated microbubbles for delivery of nitric oxide. J. Acoust. Soc. Am. **144**, 1825.

85. Corro, R., Urquijo, C.F., Aguila, O., et al. (2022). Use of nitric oxide donor-loaded microbubble destruction by ultrasound in thrombus treatment. Molecules **27**, 7218.

86. Pathak, V., Roemhild, K., Schipper, S., et al. (2022). Theranostic trigger-responsive carbon monoxide-generating microbubbles. Small **18**, 2200924.

87. Guo, W., Huang, S., An, J., et al. (2022). Ultrasound-mediated antitumor therapy via targeted acoustic release carrier of carbon monoxide (TARC-CO). ACS Appl. Mater. Interfaces **14**, 50664−50676.

88. Fix, S.M., Borden, M.A., and Dayton, P.A. (2015). Therapeutic gas delivery via microbubbles and liposomes. J. Contr. Release **209**, 139−149.

89. Chen, Y., Liang, Y., Jiang, P., et al. (2019). Lipid/PLGA hybrid microbubbles as a versatile platform for noninvasive image-guided targeted drug delivery. ACS Appl. Mater. Interfaces **11**, 41842−41852.

90. Dou, L., Yang, Y.M., You, J., et al. (2014). Solution-processed hybrid perovskite photodetectors with high detectivity. Nat. Commun. **5**, 5404.

91. Guix, M., Mayorga-Martinez, C.C., and Merkoçi, A. (2014). Nano/micromotors in (bio)chemical Sscience applications. Chem. Rev. **114**, 6285−6322.

92. Sengupta, S., Patra, D., Ortiz-Rivera, I., et al. (2014). Self-powered enzyme micropumps. Nat. Chem. **6**, 415−422.

93. Maier, A.M., Weig, C., Oswald, P., et al. (2016). Magnetic propulsion of microswimmers with DNA-based flagellar bundles. Nano Lett. **16**, 906−910.

94. Wang, W., Duan, W., Ahmed, S., et al. (2013). Small power: autonomous nano- and micromotors propelled by self-generated gradients. Nano Today **8**, 531−554.

95. Wu, Z., Li, T., Li, J., et al. (2014). Turning erythrocytes into functional micromotors. ACS Nano **8**, 12041−12048.

96. Esteban-Fernández de Ávila, B., Angsantikul, P., Ramírez-Herrera, D.E., et al. (2018). Hybrid biomembrane−functionalized nanorobots for concurrent removal of pathogenic bacteria and toxins. Sci. Robot. **3**, eaat0485.

97. Liu, F.W., and Cho, S.K. (2021). 3-D swimming microdrone powered by acoustic bubbles. Lab Chip **21**, 355−364.

98. Aghakhani, A., Pena-Francesch, A., Bozuyuk, U., et al. (2022). High shear rate propulsion of acoustic microrobots in complex biological fluids. Sci. Adv. **8**, eabm5126.

99. Lin, H., Li, S., Wang, J., et al. (2019). A single-step multi-level supramolecular system for cancer sonotheranostics. Nanoscale Horiz. **4**, 190−195.

100. Zhang, L., Yi, H., Song, J., et al. (2019). Mitochondria-targeted and ultrasound-activated nanodroplets for enhanced deep-penetration sonodynamic cancer therapy. ACS Appl. Mater. Interfaces **11**, 9355−9366.

101. Wang, X., Wang, W., Yu, L., et al. (2017). Site-specific sonocatalytic tumor suppression by chemically engineered single-crystalline mesoporous titanium dioxide sonosensitizers. J. Mater. Chem. B **5**, 4579−4586.

102. Li, D., Yang, Y., Li, D., et al. (2021). Organic sonosensitizers for sonodynamic therapy: from small molecules and nanoparticles toward clinical development. Small **17**, 2101976.

103. Xing, X., Zhao, S., Xu, T., et al. (2021). Advances and perspectives in organic sonosensitizers for sonodynamic therapy. Coord. Chem. Rev. **445**, 214087.

AUTHOR CONTRIBUTIONS

Y.J.Z. conceived the project. D.Q.H. wrote the manuscript. J.L.W. and D.Q.H. arranged the figures. J.L.W. and C.H.S. revised the manuscript.

DECLARATION OF INTERESTS

The authors have no conflicts to disclose.